Research Article Vol. 57, No. 18 / 20 June 2018 / Applied Optics 5217

applied optics

High-accuracy measurement of the focal length and distortion of optical systems based on interferometry

Guoqing Yang,[1,2] Liang Miao,[1,*] Xin Zhang,[1,2] Chuang Sun,[1,2] and Yanfeng Qiao[1]

[1]Changchun Institute of Optics, Fine Mechanics and Physics, Chinese Academy of Sciences, Changchun 130033, China
[2]University of Chinese Academy of Sciences, Beijing 100049, China
*Corresponding author: miaol@ciomp.ac.cn

Received 13 April 2018; revised 24 May 2018; accepted 24 May 2018; posted 30 May 2018 (Doc. ID 328375); published 19 June 2018

A figure measuring interferometer (FMI) method is proposed for high-accuracy measurement of the focal length and distortion of optical systems simultaneously. FMI uses the Zernike coefficients of interference fringe to identify the image point position precisely, and then measures the distance between the image points under the different fields to determine the image height. The field of view can also be accurately obtained by a precise rotating platform. Linear fitting between the field of view and the image height is used to calculate the focal length and distortion. The experimental results indicate that FMI has a relative expanded standard uncertainty of less than 0.01% for focal length and 0.02% for distortion. In brief, the proposed method is feasible for measurement of the focal length and distortion with high accuracy, promising further industrial applications.

OCIS codes: (120.3180) Interferometry; (120.0120) Instrumentation, measurement, and metrology; (120.4630) Optical inspection; (120.4820) Optical systems; (220.4840) Testing.

https://doi.org/10.1364/AO.57.005217

1. INTRODUCTION

Focal length is one of the basic characteristics of optical systems, and it is very important to measure its value for a given optical system in high precision imaging. Existing measurement methods of focal length include geometric optics and other advanced optical techniques. The classical methods based on the principles of geometric optics include nodal slide and image magnification [1]. Both of them are the most straightforward, but the measurement precision is relatively lower within 1% because of the errors in measuring sizes of the object and image. The interferometric method based on the Talbot effect and the moiré technique obtains focal length by measuring the tilt angle of the Talbot image. This method evaluates the focal length with a measurement error in the range from 0.3% to 0.05% [2–4]. In differential confocal techniques, the back-focal-distance is calculated by measuring the focus and vertex of the surface with a measurement precision of 0.01% [5], but it is not suitable for the short focal-length measurement and the back focal distance is not equal to the focal length. The process of calculating the focal length through the back focal distance may introduce other errors. Besides, a phase-shifting interferometer can obtain the back focal distance by measuring the radius of the wavefront curvature with a measurement precision of 0.02% [6]. There are many other methods of focal length measurement including the grating shearing interferometry method [7] and the fiber point diffraction longitudinal interferometry method [8]. However, their measurement accuracies need to be improved for engineering applications.

Optical distortion is defined as the distance between the real image point and the paraxial image point [9]. The fidelity of the image is characterized by optical distortion, which determines the imaging quality of the optical system. Classical methods of measuring the distortion include the accurate measuring angle and the accurate measuring length. Many other methods are based on the above methods with varying degrees of enhancement in accuracy [10–13]. For example, the distortion of the short focal length and large-field imaging system is calculated by the relationship between the distorted image and the ideal image with the precision of 0.2% [10]. Based on the diffraction formula and the paraxial optical formula, a diffraction grating is used to calculate the focal length and distortion of optical systems by measuring the transversal distances of diffraction image. The theoretical measurement accuracy reaches 0.02% [11]. Many methods exist [12,13], including those mentioned above, and are all based on the classical principle, but the accuracy still needs to be improved.

Thus, the key to improve the measurement accuracy of focal length and distortion is improving the focusing precision and

finding the accurate image points. Therefore, a method of figure measuring interferometer (FMI) is proposed in this paper to achieve accurate focusing and measuring the focal length and distortion simultaneously. The main advantage of FMI is that it identifies the precise position of image points using the Zernike coefficients of interference fringes. The accurate measuring angle and the accurate measuring length are realized as well. The focal length and distortion of optical systems can be calculated by the paraxial imaging formula with the displacements of the image points and the field angles. In addition, a new high precision measuring instrument for focal length and distortion is established using this method. A precise rotating platform and a displacement measurement interferometer (DMI) are applied to ensure the accuracy of the length measurement between different field image points. Compared to other methods, FMI has an ultrahigh measurement accuracy based on theoretical analysis of uncertainty.

2. THEORETICAL ANALYSIS AND EXPERIMENTAL SETUP

A. Measurement Principle

As shown in Fig. 1 for an infinitely conjugated system, a parallel beam of rays passes through the optical system under an angle of incidence ω. The parallel beam will be focused on an image point, according to the theory of geometrical optics, with a vertical distance y from the optical axis, providing there is no aberration. In $f-\tan\omega$ system, the relation between the distance y and the incidence angle ω can be described as [14]

$$y = f\ \tan\omega, \tag{1}$$

in which f is the focal length of the optical system. If the distance y is measured while the incidence angle ω is known in advance, the focal length f of the optical system can be easily solved with the use of Eq. (1).

As a result of the distortion existing in an actual optical system, the actual position of the image point y' is not equal to y. Suppose that field of view ω_i corresponds to the actual position of the image point y_i' $(i = 1, 2, 3 \ldots n)$. According to the least squares principle, when the sum of squares of the positional deviations under different fields is minimized, the focal length f of the optical system can be determined. It can be described as [15]

$$Q = \sum (\delta y_i')^2 = \sum (y_i' - f\ \tan\omega_i)^2, \tag{2}$$

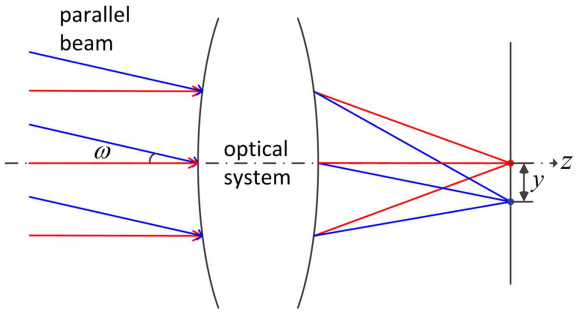

Fig. 1. Schematic of measurement device. The focal length and distortion of an optical system can be calculated from transversal distances between the different field points.

holding $\frac{\partial Q}{\partial f} = 0$, and the focal length f can be calculated as follows:

$$f = \frac{\sum (y_i' \tan\omega_i)}{\sum \tan^2\omega_i}. \tag{3}$$

A "paraxial image distance" of the image point can be expressed as

$$y_i = f\ \tan\omega_i,$$

so the distortion $\delta y_i'$ of the optical system for the given paraxial image distance can be calculated as follows:

$$\delta y_i' = y_i' - y_i. \tag{4}$$

If the position of the image point is accurately found, the distance and the field of view can be accurately measured as well, and the focal length and the distortion of the optical system can be calculated from Eqs. (3) and (4).

B. Determination of Image Point Based on Interferometry

As shown in Fig. 1, the image point is formed by the convergence of the wavefront. Assume that the image point P_1 is the curvature center of wavefront W_1, and P_2 is the curvature center of wavefront W_2, given in Fig. 2. The origin of the coordinate system is located at the curvature center P_1. Wavefront W_2 is tilted relative to wavefront W_1. When two wavefronts interfere with each other, the wavefront aberration $\Delta W(x, y, z)$ at an arbitrary point $P(x, y, z)$ on the wavefront can be described as [1]

$$\begin{aligned}
\Delta W(x,y,z) &= n_{\text{ref}} \cdot (|P_2P'| - |P_2P|) \\
&= n_{\text{ref}} \cdot \left(r - \sqrt{(x-\Delta l_x)^2 + y^2 + z^2} \right) \\
&= n_{\text{ref}} \cdot \left(r - \sqrt{r^2 + \Delta l_x^2 - 2r \cdot \Delta l_x \cdot \sin\varphi\cos\theta} \right) \\
&= n_{\text{ref}} \cdot r \cdot \left[1 - \sqrt{1 + \left(\frac{\Delta l_x}{r}\right)^2 - 2\frac{\Delta l_x}{r} \cdot \sin\varphi\cos\theta} \right] \\
&\approx \Delta l_x \cdot n_{\text{ref}} \cdot \sin\varphi\cos\theta \\
&= \Delta l_x \cdot \rho \cdot \text{NA} \cdot \cos\theta \\
&= a_x \cdot Z_1,
\end{aligned} \tag{5}$$

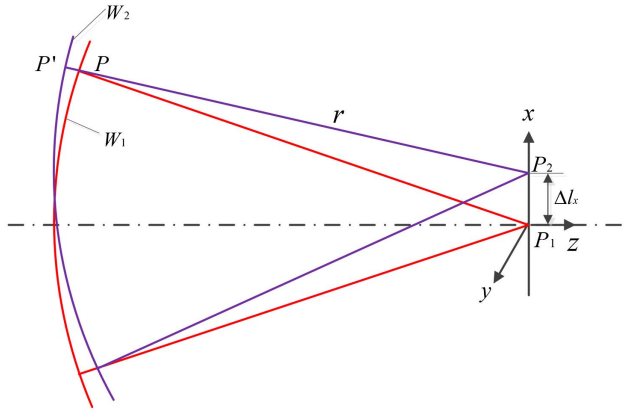

Fig. 2. Geometry analysis for wavefront aberration between wavefront W_1 and W_2.

where ρ is the normalized radius, θ is the azimuth angle at an arbitrary point P in the x-y plane, NA is the numerical aperture of the wavefront, n_{ref} is the refractive index of the medium where the wavefront is located in, φ is the aperture angle, Δl_x is the offset distance between point P_1 and point P_2, and r is the curvature radius of wavefront W_1 and W_2. The magnitude of ΔW decided with the offset distance Δl_x can also be expressed by a Zernike polynomial. Z_1 is the x tilted term of the Zernike polynomials, and a_x is the corresponding coefficient.

The following formula can be obtained from Eq. (5),

$$\Delta l_x = \frac{a_x}{\text{NA}}, \tag{6}$$

indicating that the offset of the image point along the x axis can be expressed by the coefficient a_x of Zernike tilted term. The following formula can be obtained similarly,

$$\Delta l_y = \frac{a_y}{\text{NA}}, \tag{7}$$

in which a_y is the coefficient of the y tilted term Z_2 of Zernike polynomials, and Δl_y is the offset distance of the image point along the y axis. It shows that the offset of the image point along the y axis can be expressed by the coefficient a_y of the Zernike tilted term. The coefficients a_x and a_y can be obtained from the interference fringe, when ΔW is fitted by Zernike polynomials. If the point P_2 is known and can be moved by a motion control device, the position of the image point P_1 can be found accurately based on Eqs. (6) and (7).

C. Overview of the Measurement System

Figure 3 shows the schematic of an experimental setup for an infinitely conjugated system, and the measurement process is as follows. The laser light is emitted by a monochromatic point source to produce a divergent beam. The divergent beam passes through a beam splitter and is collimated into a parallel beam with a collimating lens. The parallel beam is divided by a reference flat into two components: the first component, called the reference beam, is reflected by the reference flat, and the second component, called the measuring beam, transmits through the reference flat. The reference beam retraces along the same way, and then it is reflected by the beam splitter into a charge-coupled device (CCD) camera. The measuring beam is reflected by a reflector into the testing optical system and then focuses on an image point. When the image point is aligned with the curvature center of the reflection sphere (RS), the measuring beam reflected by surface of the RS retraces along the same way, and then it is also reflected by the beam splitter into the CCD camera. An interference pattern is observed.

When the reflector controlled by a precise rotating platform turns a certain angle ω_0, the field angle of the incidence beam changes $2\omega_0$, and the image point moves a certain distance. In the case of ideal imaging, the image point moves along a straight line under different fields. The curvature center of the RS controlled by a motion control device follows and overlaps the image point, and the beam backtracks to the CCD camera. An interference pattern is observed under another field of view. The distance from the curvature center of the RS can be accurately measured by a DMI system. From all of the above, the position of the image point that is converged by the parallel beam passing through the optical system under different fields can be found.

D. Measurement Procedure

The measurement system aims to obtain the field of view and the actual position of the image point. The demonstration of real measurement is shown in Fig. 4. Each scan of the interferometer aiming to measure the full field is carried out by changing various angles of the reflector and positions of the RS via the precise rotating platform and the motion control device, respectively.

The measurement procedure is explained in detail in Fig. 5. The initial position is at the field center of the optical system. According to the theory of interference [1], the condition of focusing is that the interference fringe must be null so that the image point and the curvature center of the RS overlap at every single field angle. As described in Section 2.B, the position of image point (point P_1 in Fig. 2) can be determined accurately by controlling the curvature center of the RS (point P_2 in Fig. 2). In other words, corresponding coefficients of Zernike tilted terms of the interference fringe should be very small. Such an image point position can be called a null point position. By means of turning the precise rotating platform, a

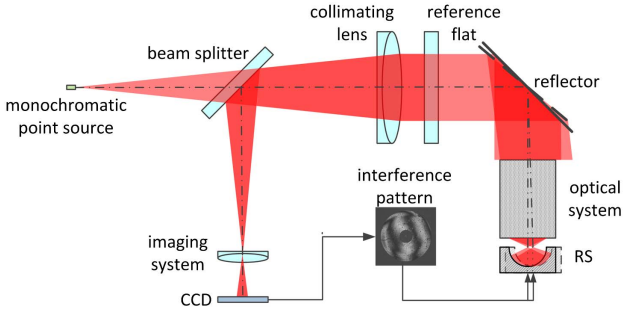

Fig. 3. Schematic of an experimental setup. Interference pattern can be observed under different fields.

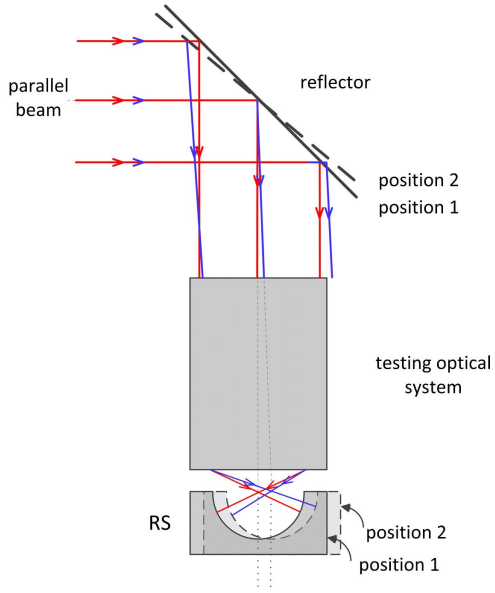

Fig. 4. Measurement procedure. The red light is at position 1 and the blue light is at position 2.

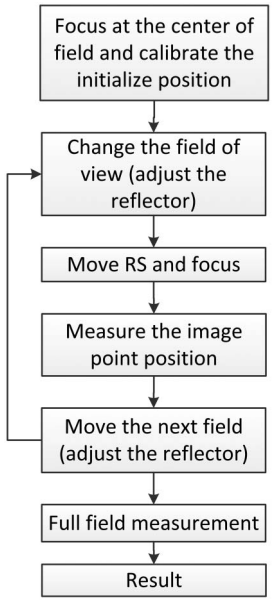

Fig. 5. Flow chart of measurement.

series of field angles can be obtained, and the corresponding null point position can be measured. After that, an experimental result of the measurement system is shown in Chapter 4 according to the measurement principle as stated above.

3. MEASUREMENT UNCERTAINTY ANALYSIS

According to the theoretical analysis, the position of the image point is one of the main factors that determines the measurement accuracy. The aberration of the optical system affects the position of the image point. The following formula can be expressed by the theory of the third-order aberration for the object at infinity [9,11],

$$\delta y' = -\frac{1}{2}(S_2 \cdot \mathrm{NA}^2 \tan\omega + S_5 \tan^3\omega), \tag{8}$$

where $\delta y'$ is the transverse ray aberration of the image point in the paraxial image plane, S_2 is the coefficient of coma, S_5 is the coefficient of distortion, ω is the angle of the field, and NA is the numerical aperture of the optical system in the image space. It can be shown that the coma and the distortion of the optical system affect the determination of the position of the image point. To reduce the measurement error, the optical system to be measured should be a small aberration optical system. The wave aberration RMS of the optical system measured in this experiment is 0.06λ RMS, better than the diffraction limit, and the field of view is ± 4 deg, so the measurement results of the tested optical system can be considered nearly unaffected by the aberrations [11].

It is known from the measurement principle that the focal length and distortion can be calculated by the field angle ω and the position of image point y', so the influence factors of the uncertainty in the measurement originate from the measurement errors of the field angle and the position of the image point.

A. Uncertainty Caused by the Incidence Angle ω

In the measurement system, a precise angle dividing table with a rotating angle error of 1 μrad is used to change the incidence angle. The corresponding rotating angle error of the field is 2 μrad. According to the uniform distribution, u_ω caused by ω can be described by type B uncertainty, as follows:

$$u_\omega = \frac{1}{\sqrt{3}} \times 2\ \mu\mathrm{rad} \approx 1.155\ \mu\mathrm{rad}. \tag{9}$$

B. Uncertainty Caused by the Position of the Point y'

The position of the image point is measured by DMI. Its errors include measurement repeatability error caused by some random factors, null point position determination error, axial misalignment error, and displacement measuring error.

1. Uncertainty Caused by Measurement Repeatability

The measurement of DMI can be influenced by some random factors, such as environmental disturbances, deadpath error, and thermal expansion coefficient, resulting in the uncertainty of measurement repeatability. The errors can be described as standard deviation σ_{randow} of several repeated measurements. Therefore, the uncertainty u_A caused by measurement repeatability can be described by type A uncertainty, as follows:

$$u_A = \sigma_{\mathrm{random}}. \tag{10}$$

2. Uncertainty Caused by the Null Point Position Error

As previously mentioned, the accurate null point position is determined by the coefficients of Zernike tilted terms of interference fringe. According to the theory of interference based on Eqs. (6) and (7), the following formula can be obtained,

$$\sigma_l = \frac{\sigma_a}{\mathrm{NA}}, \tag{11}$$

where σ_l is the offset of the image point, σ_a is the maximum permissible value of Zernike coefficients a_x and a_y, and NA is the numerical aperture of the optical system. Assuming the error obeys the uniform distribution, the uncertainty u_l caused by the null point position error can be described by type B uncertainty, as follows:

$$u_l = \frac{\sigma_l}{\sqrt{3}}. \tag{12}$$

3. Uncertainty Caused by Axial Misalignment Error

As shown in Fig. 6, in the measurement system, axis m of the motion direction, axis s of the measured surface normal, and axis d of DMI should be aligned, but the deviation angles between them more or less exist in practice. Suppose that the angle between axis s and axis d is α, then the angle between axis s and axis m is β. Then the axial misalignment error contains cosine error and Abbe error [16].

Cosine error is a linear quantity that varies with the measured displacement. If α and β cannot be negligible, cosine error can be described as [16]

$$\sigma_{\mathrm{cosine}} = y'(1 - \cos\alpha\cos\beta), \tag{13}$$

where y' is the displacement of the image point movement. The uncertainty u_{cosine} can be described by type B uncertainty, as follows:

$$u_{\mathrm{cosine}} = \frac{\sigma_{\mathrm{cosine}}}{\sqrt{3}}. \tag{14}$$

Abbe error is caused by the inclination of the measured surface during the movement. If the amount of tilt is constant

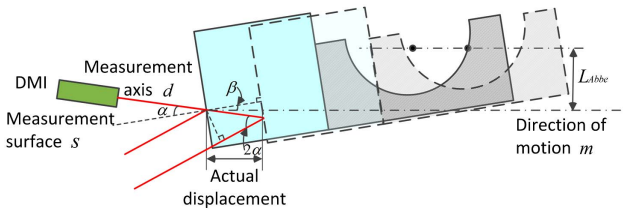

Fig. 6. Axial misalignment error contains cosine error and Abbe error in the measurement system.

during the movement, Abbe error does not exist. Otherwise it can be described as [16]

$$\sigma_{\text{Abbe}} = L_{\text{Abbe}} \tan \sigma_\beta, \tag{15}$$

where L_{Abbe} is the Abbe arm length. σ_β is the variation of β. The uncertainty u_{Abbe} caused by β can be described by type B uncertainty, as follows:

$$u_{\text{Abbe}} = \frac{\sigma_{\text{Abbe}}}{\sqrt{3}}. \tag{16}$$

4. Uncertainty Caused by Displacement Measuring Error

In the measurement system, the displacement is measured using the laser interferometric measurement system produced by Shanghai Jian Hai Semiconductor Equipment Co. Ltd. (JHSE). Its measurement error without environmental fluctuations mainly depends on the accuracy of the laser wavelength, which is ±0.1 ppm, so the following formula can be obtained,

$$\sigma_d = 1 \times 10^{-7} \times y', \tag{17}$$

in which the uncertainty u_d caused by the displacement measuring error can be described by type B uncertainty, as follows:

$$u_d = \frac{\sigma_d}{\sqrt{3}}. \tag{18}$$

Considering the above uncorrelated uncertainty elements, the combined uncertainty $u_c(y')$ can be described as follows [15]:

$$u_c(y') = \sqrt{u_A^2 + u_l^2 + u_{\text{cosine}}^2 + u_{\text{Abbe}}^2 + u_d^2}. \tag{19}$$

C. Measurement Uncertainty of the Focal Length f

According to the law of uncertainty propagation based on Eq. (3), the uncertainty $u(f)$ can be described as [15]

$$u(f) = \sqrt{\sum \left(\frac{\partial f}{\partial \omega_i} u_\omega\right)^2 + \sum \left(\frac{\partial f}{\partial y_i'} u_c(y')\right)^2}, \tag{20}$$

where

$$\frac{\partial f}{\partial \omega_i} = \frac{y_i' \sum \tan^2 \omega_i - 2 \tan \omega_i \sum y_i' \tan \omega_i}{(\cos \omega_i \sum \tan^2 \omega_i)^2},$$

$$\frac{\partial f}{\partial y_i'} = \frac{\tan \omega_i}{\sum \tan^2 \omega_i}.$$

The expanded standard uncertainty for $k = 2$ with the confidence probability of 0.95 is

$$U(f) = 2u(f). \tag{21}$$

D. Measurement Uncertainty of the Distortion $\delta y_i'$

It is known from Eq. (4) that the distortion $\delta y_i'$ is residuals of the linear fitting curve, so the estimation of uncertainty $u(\delta y_i')$ in determination of the paraxial image distance y_i and the actual image distance y_i' can be described as follows [15]:

$$u(\delta y_i') = \sqrt{u(y_i)^2 + u(y_i')^2}. \tag{22}$$

$u(y_i)$ is the uncertainty of the paraxial image distance y_i, which is linearly fitted by the least square method, so it can be ignored. $u(y_i')$ is the uncertainty of the actual image distance y_i', which is measured by DMI. The linear error in it does not contribute to the uncertainty of distortion, so

$$u(y_i') = \sqrt{u_A^2 + u_l^2 + u_{\text{Abbe}}^2 + u_d^2}.$$

The expanded standard uncertainty for $k = 2$ with the confidence probability of 0.95 is

$$U(\delta y_i') = 2u(\delta y_i'). \tag{23}$$

4. EXPERIMENTS AND MEASUREMENT RESULTS

Based on the measurement principle shown in Fig. 3, the main structure of the measurement system is designed as shown in Fig. 7. It includes an interferometer measurement system, an angular adjustment system, a distance measuring system, and a kinematic position system.

The experimental setup shown in Fig. 7 is established to measure the microscope objective. Its basic design parameters are as follows: the focal length is 14.7360 mm and the distortion is 78 nm. A 4-inch interferometer produced by ZYGO with a wavelength of 632.8 nm is used to produce the interferograms. A precise angle dividing table WDFT-720B produced by Jiujiang Jingda Measurement Technology Co. Ltd. is used to adjust the incidence angle with the error of 2 μrad. A RS produced by ZYGO is used to reflect the measuring beam. Its basic parameters are that F-number is 0.51 and R is 12.7 mm. A six-axis-parallel kinematic positioning system of Newport is used to move the RS with a step of 100 nm. A laser interferometric measurement system produced by JHSE is used as a DMI system. The core component is the dual-frequency laser, which is Agilent's 5517DL.

The experiments are conducted under the following conditions: the temperature is 22 ± 0.5°C, the pressure is 99 ± 2 kPa, and the relative humidity is (40 ± 5)%. During measurement data processing, the position of focal points should be measured within a few minutes to reduce the influence of environmental disturbances.

In the experiment, nine fields ($i = 1, 2, 3 \ldots 9$) are set from −4 to +4 deg, and the corresponding displacements are measured by the DMI system. One of the measurement results is shown in Table 1. The relationship between the displacement and the field angle is close to linear. Thus, the focal length f and the maximum distortion $\delta y_i'$ of the test microscope objective calculated from Eqs. (3) and (4) are 14.7579 mm and 184 nm, respectively.

Five measurement results of the focal length and distortion are shown in Figs. 8 and 9, respectively. The average and standard deviation of the focal length are 14.7583 mm and 483 nm, respectively. The average and standard deviation of the distortion are 143 nm and 74 nm, respectively.

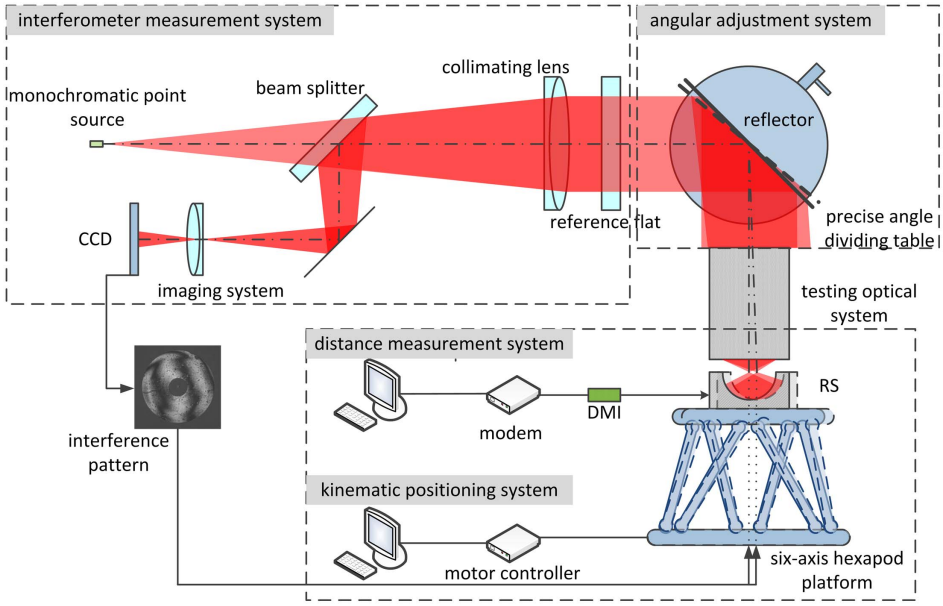

Fig. 7. Main structure of measurement system.

From Eq. (10), u_A can be calculated by the five measurements, and u_A is 65 nm. For a high-accuracy measurement system, the null point position error σ_a can be controlled within $\pm 0.1\lambda$ by adjusting the RS. u_l can be calculated as 37 nm according to Eqs. (11) and (12). Angle α can be controlled within 10′, angle β can be controlled within 10″, and Abbe arm length L_{Abbe} can be controlled within 2 mm during the installation process. The variation σ_β of β is measured by an autocollimator within 2″ in the process of experiment. Therefore, the uncertainty u_{cosine} and u_{Abbe} calculated from Eqs. (13), (14), (15), and (16) are 5 nm and 11 nm, respectively. The field diagonals of the test optical system is 2.08 mm; thus, the displacement y' is small enough so that u_d can be ignored. Substituting these values into Eq. (19), the combined uncertainty $uc(y')$ is calculated as 76 nm. The standard uncertainty $u(f)$ is calculated from Eq. (20), as follows:

$$u(f) = 576 \text{ nm}. \tag{24}$$

The expanded standard uncertainty for $k = 2$ with the confidence probability of 0.95 is

$$U(f) = 2u(f) = 1152 \text{ nm}, \tag{25}$$

so the measurement result of the focal length is

$$f = 14.7583 \pm 0.0012 \text{ mm}, \qquad p = 0.95. \tag{26}$$

The relative expanded standard uncertainty of the focal length is

$$U_{\text{rel}}(f) = \frac{U(f)}{f} \times 100\% = 0.0078\%. \tag{27}$$

Substituting $u(y_i)$ and $u(y_i')$ into Eq. (22), the standard uncertainty $u(\delta y_i')$ is obtained as

$$u(\delta y_i') = 76 \text{ nm}. \tag{28}$$

The expanded standard uncertainty for $k = 2$ with the confidence probability of 0.95 is

$$U(\delta y_i') = 2u(\delta y_i') = 152 \text{ nm}, \tag{29}$$

so the result of the measurement of the distortion is

$$\delta y_i' = 143 \pm 152 \text{ nm}, \qquad p = 0.95. \tag{30}$$

Table 1. Null Point Position Under Different Fields

FOV ω (degree)	Displacement y' (mm)
−4	−1.03179
−3	−0.77344
−2	−0.51542
−1	−0.25762
0	0
1	0.25768
2	0.51548
3	0.77353
4	1.03196

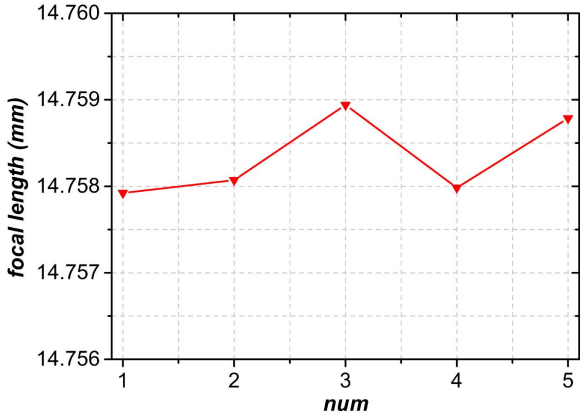

Fig. 8. Five measurement results of focal length.

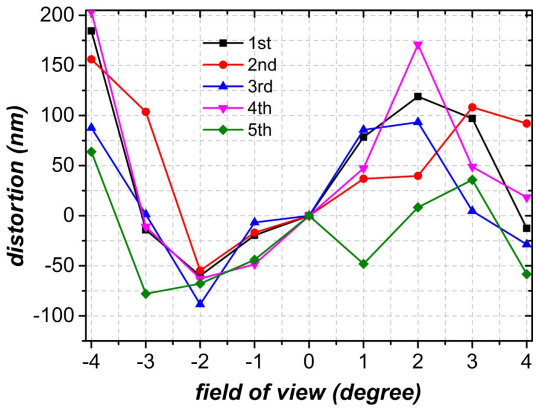

Fig. 9. Five measurement results of distortion under different fields.

The relative expanded standard uncertainty of the distortion is

$$U_{\text{ref}}(\delta y_i') = \frac{U(\delta y_i')}{y'} \times 100\% = 0.0146\%, \tag{31}$$

with y' as the half field height 1.04 mm.

5. CONCLUSION

The paper presents a method for measuring the focal length and distortion of optical systems simultaneously based on interferometry. Compared to the other methods, FMI uses the Zernike coefficients of interference fringes to identify the image point position precisely, and measures the image height and the field angle with high accuracy as well. The focal length and the distortion of optical systems calculated through theoretical analysis and calculation are performed, and the uncertainties of measurement are also studied. Preliminary experiments show that the relative expanded standard uncertainty of the focal length for $k = 2$ is 0.0078%, and the relative expanded standard uncertainty of the distortion for $k = 2$ is 0.0146%; thus, the precision is improved remarkably. And the measurement results coincide with the design values. Therefore, the proposed method is feasible for laboratory testing with high accuracy and for industrial applications as well.

Funding. National Youth Foundation of China (61605202).

Acknowledgment. We thank GeOptics Sequencing Equipment Co. Ltd. for the use of its equipment.

REFERENCES

1. D. Malacara, *Optical Shop Testing* (Wiley, 2007).
2. Y. Nakano and K. Murata, "Talbot interferometry for measuring the focal length of a lens," Appl. Opt. **24**, 3162–3166 (1985).
3. P. Singh, M. S. Faridi, C. Shakher, and R. S. Sirohi, "Measurement of focal length with phase-shifting Talbot interferometry," Appl. Opt. **44**, 1572–1576 (2005).
4. S. Trivedi, J. Dhanotia, and S. Prakash, "Measurement of focal length using phase shifted moiré deflectometry," Opt. Lasers Eng. **51**, 776–782 (2013).
5. Z. Li, L. Qiu, W. Zhao, and Q. Zhao, "Laser multi-reflection differential confocal long focal-length measurement," Appl. Opt. **55**, 4910–4916 (2016).
6. T. Parham, T. J. McCarville, M. A. Johnson, and C. Kiikka, "Focal length measurements for the national ignition facility large lenses," in *Optical Fabrication and Testing (OFT)* (2002), paper OWD8.
7. F. Lei and L. K. Dang, "Measuring the focal length of optical-systems by grating shearing interferometry," Appl. Opt. **33**, 6603–6608 (1994).
8. L. Chen, J. Hao, Z. Chen, and X. Guo, "Focal length measurement by fiber point diffraction longitudinal interferometry," Opt. Commun. **322**, 48–53 (2014).
9. A. Miks and J. Novak, "Dependence of camera lens induced radial distortion and circle of confusion on object position," Opt. Laser Technol. **44**, 1043–1049 (2012).
10. J. Lin, M. Xing, D. Sha, D. Su, and T. Shen, "Distortion measurement of CCD imaging system with short focal length and large-field objective," Opt. Lasers Eng. **43**, 1137–1144 (2005).
11. A. Miks and P. Pokorny, "Use of diffraction grating for measuring the focal length and distortion of optical systems," Appl. Opt. **54**, 10200–10206 (2015).
12. X. Yu, Q. Li, X. Jiang, F. Wang, and H. Wang, "Distortion measurement and calibration technology research of automatic observing and aiming optical system based on CCD," Proc. SPIE **7283**, 728319 (2009).
13. X. Yu, Q. Li, X. Jiang, F. Wang, and H. Wang, "Research on distortion measurement and calibration technology for TV-seeker," Proc. SPIE **7511**, 75111U (2009).
14. M. Born and E. Wolf, *Principle of Optics* (Oxford University, 1964).
15. M. Grabe, *Measurement Uncertainties in Science and Technology* (Springer, 2014).
16. L. A. Selberg, "Radius measurement by interferometry," Opt. Eng. **31**, 1961–1966 (1992).